

Compressed Acquisition Method for Global Navigation Satellite System Signal

Yanxin Yao, Minling Zhu

School of Information and Communication Engineering,
Beijing Information Science and Technology University, China
Yanxin_buaa@126.com, zhuminling@bistu.edu.cn

Abstract

In the acquisition of Global Navigation Satellite System (GNSS) receivers, the correlation process has computing-resource requirements. The paper introduces compressed sensing theory to GNSS signal acquisition and studies the methods of measuring the compressive correlation values and reconstructing acquisition information. First, the mathematical expressions of compressed parallelized correlation measurements are deduced. Second, the compressed parallelized correlation-measurement values are decomposed into the sensing matrix and the sparse signal containing the acquisition information. Finally, the sparse signal is reconstructed and detected to further estimate the acquisition information. The calculation cost and detection performance of the compressed acquisition-processing method are analyzed. A real-time experiment shows that the method is feasible. Simulations show the probability of successful acquisition under different signal-to-noise ratios and dimension-reduction conditions, with a reduced calculation cost compared to the serial acquisition method. Though the detection performance is slightly degraded compared to the conventional acquisition method, low sampling rate and low digital-computation cost will be achieved when realized with a correlation structure in the analog domain. The method has certain application value.

Keywords: Compressed sensing, Global navigation satellite system, Code division multiple access, Acquisition, Detection performance, Reconstruction

1 Introduction

Through a search process, acquisition can identify the satellite pseudo-random noise (PRN) code number of the received signal and roughly estimate the phase of the satellite PRN code and the Doppler frequency of the carrier [1, 2]. When the Global Navigation Satellite System (GNSS) receiver is in the mode of blind acquisition and cold start, the uncertainty of the

satellite signal may cover all the satellites, all the possible frequency ranges and all the code phases [3]. The acquisition methods could eliminate this uncertainty. The acquisition methods classified into serial search, parallel search, etc. [4-7] Acquisition-correlation operations occupy most of the computations in the processing procedure of the GNSS receiver. The resolution of code acquisition is at least 1/2 a chip, and the frequency resolution is generally less than 500 Hz and is related to the correlation-integration time. For 1023 chips of Global Positioning System (GPS) C/A code, the general ground-base and air-base receivers need to address a Doppler frequency offset search range of -6 kHz~6 kHz, and at least 2046*25 correlators are needed for each satellite [4]; for Doppler frequency offset search range of -10 kHz~10 kHz, at least 2046*41 correlators are needed for each satellite.

Serial acquisition is serial search of the code phases and Doppler frequencies with a digital correlator consuming time and a large amount of computation cost. Some of the parallel correlation methods, such as the matched-filter scheme and fast Fourier-transform (FFT) acquisition scheme [4, 6], can accelerate the acquisition speed, but the total calculation cost of the matched-filter method is not reduced. For an accumulation time of 1 ms in the case of C/A code, the matched-filter scheme corresponds to 41 sliding, matching or correlation operations with 2046 points, equal to the Serial acquisition.

However, some parallel correlation methods, such as The FFT acquisition scheme, greatly reduce the calculation cost [4]. At present, the methods of reducing the calculation cost also include the extended replica-folding search technique (XFAST) acquisition method [7] and the Partial Matching Filter FFT (PMF-FFT) method [6]. Choosing an appropriate number of folding segments can improve the search efficiency and reduce the calculation cost.

Compressed sensing is the latest development of science and technology [9, 10]. Compressed sensing can reduce the sampling rate and the calculation cost of

the digital-processing procedure. This paper focuses on using compressed sensing to realize acquisition.

We can construct a suitable sparse-signal model or redundant dictionary with the technology of compressed sensing to process different signals [11, 12] and recover the key information in the signal structure using far fewer measurements than conventional methods [13]. Hansen has applied compressed sensing in GNSS. He uses classic random binary matrices to measure Global positioning system (GPS) signal, and reconstruct signal based on the Reduce multiple measurement vector and boost (ReMbo) algorithm, which needs a lot of computations [14]. Seung Hyun Kong [15] proposes a structured measurement matrix to measure signal with two stages, and reconstruct signal using Walsh Hadmard transform, but two stages compressed sensing will introduce too much noise.

This paper introduces a new model to utilize compressed sensing to realize the acquisition of GNSS signals. We obtain the acquisition information by the steps of compressive measurement of correlation values, sparse representation of measurements, design of the sensing matrix and recovery of key information. The reconstruction could use the relatively simple Orthogonal Matching pursuit (OMP) algorithm. The computational complexity and acquisition performance of compressed acquisition for GNSS signals are analyzed. Experiments are carried out to obtain results on the reconstruction of sparse signals and the probability of successful acquisition under various signal-to-noise ratios (SNRs) and dimension-reduction ratios. The compressed acquisition method is compared

with conventional acquisition methods.

The paper is organized as follows. Section 2 describes the proposed compressed acquisition method and introduces the compressed acquisition structure, including the compressed parallel-correlation unit and the signal-reconstruction and detection unit. The calculation cost is analyzed in Section 2.3, and the acquisition-detection performance is analyzed and compared with those of conventional acquisition methods in Section 2.4. Section 3 presents the experiments, along with simulated and real data, to validate the method. Section 4 concludes the paper.

2 Compressed Acquisition

Due to the good auto-correlations and cross-correlations of pseudo-random sequences of satellite signals, among all the satellites, frequency grids and uncertain code chips to be searched, a large peak value will be obtained only when the correct code phase of a visible satellite and the correct frequency are used to dispread and demodulate the received signal; otherwise, after disspreading and demodulation, the obtained correlation values are much smaller and the acquisition-correlation peak value can be ignored. Therefore, the correlation values satisfy the sparsity property in a certain sense. Utilizing this characteristic of satellite-signal acquisition, we design a system to carry out acquisition with compressed sensing; its structure is depicted in Figure 1.

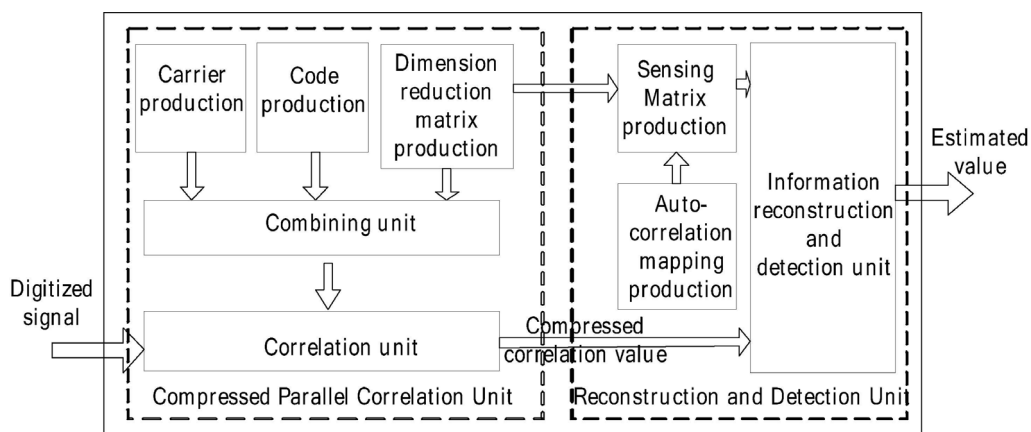


Figure 1. Compressed acquisition system structure

The digital intermediate frequency (IF) signal is obtained and processed after the satellite-navigation signal received by the antenna is low-noise amplified, filtered, down-converted and sampled by a conventional A/D converter. The main purpose is to disspread and demodulate the digital IF signal with fewer channels (correlation branches) and carry out acquisition detection to obtain the correct estimations of satellite PRN number, carrier frequency grid and code phase. This can reduce the calculation cost of

correlation and can replace the traditional correlator for disspreading and demodulation. As shown in Figure 1, the signal-processing module that accomplishes acquisition consists of a compressed parallel-correlation unit and an acquisition and detection unit.

2.1 Compressed Parallel Correlation

An analog IF signal is converted to a digital IF signal through A/D conversion, which is defined as

$$r(n) = A_i D_i(nT_s) C_i(nT_s - \tau_{ni}) \cos[(w_0 + w_{di})(nT_s - t_{oi}) + \phi_{ni}] \quad (1)$$

For convenience, (1) represents only the signal of the i th satellite, $i=1, 2, \dots, I$; n is the sampling number, $n=1, 2, 3, \dots$; T_s is the sampling interval; $C_i(\bullet)$ is the spread-spectrum code sequence of satellite i ; $D_i(\bullet)$ is the navigation data; w_0 is the digital IF frequency; w_{di} is the Doppler shift; t_{oi} is the reference time; τ_{ni} is the initial code phase at reference time t_{oi} ; and ϕ_{ni} is the initial phase of the carrier wave at reference time t_{oi} .

In serial acquisition and parallel acquisition methods, N times of correlation (N correlation channels) are needed to search all code phases, and $T_{accu}/T_s = N$. T_{accu} is the correlation-integration time. Now, we construct the compressed correlation function $\psi_p(i, k)$ of each branch (each channel). Only P branches are retained after compression, so we only need to perform P correlation operations to obtain the compressed measurements $c_p(i, k)$. The compressed measurements are decomposed into the sensing matrix and sparse vector in Section 2.2, so we can recover the information needed for acquisition from the compressed measurements.

As shown in Figure 1, the carrier-production unit generates a local complex carrier $carr(k, n)$ with a certain frequency search interval:

$$carr(k, n) = \exp[j(w_0 + k\Delta w)(nT_s - t_{oi}) + j\hat{\phi}_{ni}], \quad (2)$$

where Δw is the frequency search interval; k is the search frequency bin index; k is an integer between $-K$ and K , $K = \lfloor \frac{w_{\max}}{\Delta w} \rfloor + 1$; w_{\max} is the maximum possible absolute value of the Doppler frequency; $\lfloor \bullet \rfloor$ denotes the floor operation; and $\hat{\phi}_{ni}$ is the estimate of ϕ_{ni} .

The code-production unit produces local code $code(i, h, n) = C_i(nT_s - hT_s)$ for each satellite, with different delays. hT_s is the delay of the local-code phase at reference time t_{oi} .

The dimension-reduction matrix-production unit generates dimension-reduction matrix $A_{P \times N}$ in a certain way with dimension $P \times N$, and a_{ij} is the (i, j) th element of $A_{P \times N}$.

The combining unit combines carrier $carr(k, n)$ and code $code(i, h, n)$ with the dimension-reduction matrix A in the following way. The correlation function $\psi_p(i, k)$ is generated for each branch:

$$\psi_p(i, k) = \sum_{h=1}^N \alpha_{p,h} \cdot coca(i, h, n, k) \quad (3)$$

where $carr(i, h, n, k) = carr(k, n) = code(i, h, n)$, $p = 1, 2, \dots, P$ and $n = 1, 2, \dots, N$.

The dimension-reduction matrix is the measurement matrix in compressed-sensing theory [11, 12]. P is much smaller than N but is greater than some threshold value that depends on the type of measurement matrix and the sparsity e . For the acquisition of multiple satellites, ideally four satellites are enough to achieve positioning. However, considering the Geometric Dilution of Precision (GDOP) and other properties, such as continuity and availability, generally, more visible satellites are acquired and tracked to provide more information for high-performance positioning. Taking the impact of interference, multipaths or other special applications into account, we set e after considering various factors synthetically [16].

In compressed-sensing theory, we can choose a random Gaussian measurement matrix, a random Bernoulli measurement matrix or a deterministic stochastic matrix (polynomial measurement matrix) [17]. If we choose a random Gaussian measurement matrix, only $P \gg c \cdot e \cdot \log_2(N/e)$ measurements are needed to satisfy the restricted-isometry property (RIP) with high probability, where c is a very small constant [10, 13].

The correlation operation is performed between the correlation function $\psi_p(i, k)$ and the input digital IF signal $r(n)$, and then, we can obtain the compressed correlation value $c_p(i, k)$ for each branch:

$$c_p(i, k) = \sum_{n=1}^N [r(n) \cdot \psi_p(n)], \quad (4)$$

where $p = 1, 2, \dots, P$ indicates the label of the compressed channel. For specific (i, k) , $c_p(i, k)$, ($p = 1, 2, \dots, P$) constitutes a vector of size $P \times 1$.

The number of samples in (4) for correlation is N , so we can derive

$$c_p(i, k) = \sum_{h=1}^N \left\{ \alpha_{p,h} \cdot \frac{1}{2} A_i D_i \frac{T_{accu}}{T_s} R_i(\tau_{ni} - hT_s) \cdot s_a \left[\frac{1}{2} (k\Delta w - w_{di}) T_{accu} \right] \cdot \exp[-j(\phi_{ni} - \hat{\phi}_{ni})] \right\} + noi_2(p) \quad (5)$$

where $R_i(\tau) = [T_s \sum_{n=1}^N C_i(nT_s) C_i(nT_s - \tau)] / T_{accu}$ is the autocorrelation function of the GNSS code and $s_a(x) = \sin(x)/x$. This is the processing procedure for

a specific frequency bin of a specific satellite. It can search all code chips one time. For other frequency bins of other satellites, we can perform the processing using a similar approach.

2.2 Signal Reconstruction and Acquisition Detection

Let $c_p(i, k)$, ($p=1, 2, \dots, P$) be an element of the measurement vector \mathbf{y} in compressed sensing. To simplify the statement, we denote the measurement vector by $\mathbf{y} = [c_1, c_2, \dots, c_p]$ regardless of the values of i, k . To recover the sparse signal, we need to design a proper sensing matrix \mathbf{B} to obtain the sparse vector \mathbf{s} .

$$\mathbf{y} = \mathbf{B}\mathbf{s} \tag{6}$$

\mathbf{B} and \mathbf{s} correspond to the sensing matrix Θ and the sparse vector α , whose sparsity is e . (8) is equivalent to $\mathbf{y} = \Theta\alpha$ in compressed-sensing theory, where \mathbf{y} represents the measurements, and sensing matrix Θ satisfies the RIP condition [11]. Thus, c_p is decomposed into

$$c_p(i, k) = \sum_{h=1}^N b_{p,h} s_{i,k}(h) \tag{7}$$

where $b_{p,h}$ is the (p, n) th element of sensing matrix \mathbf{B} , $p=1, 2, \dots, P$ and $n=1, 2, \dots, N$, and $s_{i,k}(h)$, $h=1, 2, \dots, N$, are the elements of the sparse vector \mathbf{s} .

Comparing (7) with (5), we can see that

$$c_p(i, k) = \sum_{h=1}^N \left[\sum_{n=1}^N \alpha_{p,n} \cdot R_i(nT_s - hT_s) \right] \cdot s_{i,k}(h) \tag{8}$$

Therefore, for h' satisfying $h'T_s = \tau_{ni}$,

$$s_{i,k}(h') = \frac{1}{2} A_i D_i \frac{T_{accu}}{T_s} S_a \left[\frac{1}{2} (k\Delta w - w_{di}) T_{accu} \right] \cdot \exp[-j(\hat{\phi}_{ni} - \hat{\phi}_{ni})] \tag{9}$$

For h' satisfying $h'T_s \neq \tau_{ni}$, $s_{i,k}(h') = 0$. (10)

According to (9), $b_{p,h}$ can be calculated as follows,

$$b_{p,h} = \sum_{n=1}^N \alpha_{p,n} \cdot R_i(nT_s - hT_s), h=1, 2, \dots, N \tag{11}$$

The value of $s_{i,k}(h')$ indicates the signal accumulation amplitude of the i th satellite in the k th frequency bin for initial code phase corresponding to time $h'T_s$. When $s_{i,k}(h')$ is larger than the threshold, the signal acquisition is fulfilled to obtain information for i, k and $h'T_s$.

Therefore, we design the reconstruction and

detection unit in Figure 1. The reconstruction and detection unit is composed of the sensing-matrix production unit, correlation-mapping production unit, and information-reconstruction and detection unit. First, the sensing-matrix production unit generates sensing matrix \mathbf{B} according to the periodic auto-correlation function $R_i(nT_s - hT_s)$ of the GNSS code and the dimension-reduction matrix \mathbf{A} , which was output by the compressed parallel-correlation unit. The cross-correlation mapping production unit produces the cross-correlation function of the code sequences with various code phase differences:

$$R_i(hT_s) = \frac{T_s \sum_{n=1}^N C_i(nT_s) C_i(nT_s - hT_s)}{1023T_c} \tag{12}$$

Each element in matrix \mathbf{B} is computed according to (13). The information-reconstruction and detection unit reconstructs and detects the signal according to the compressed correlation function $c_p(i, k)$ of sensing matrix \mathbf{B} . For this, reconstruction algorithms of compressed sensing could be used.

Compressed sensing theory can be used to obtain the sparse solution of the signal, and there are many compressed sensing reconstruction algorithms from which to choose, such as Matching Pursuit (MP), Orthogonal Matching pursuit (OMP), and CoSaMP [13, 18-20].

We recover the $N \times 1$ vector $\mathbf{s}_{i,k} = [s_{i,k}(1), s_{i,k}(2), \dots, s_{i,k}(N)]^T$ using the reconstruction algorithm. According to the expression principle of sparse signals, we should find the e numbers whose absolute values are relatively larger than those of the others. We find the largest amplitude values $s_{i,k}(\hat{g}v)$ ($\hat{g} \in \{1, 2, \dots, N\}$, $v \in \{1, 2, \dots, e\}$) in $s_{i,k}(1), s_{i,k}(2), \dots, s_{i,k}(N)$. If the amplitude value is larger than the preset detection threshold, this indicates that the signal of satellite i_v is detected in frequency bin k_v . The absolute value $|s_{i,k}(\hat{g}v)|$ indicates the relative amplitude of the signal, and the location $\hat{g}v$ indicates the delay of the code phase $\hat{g}vT_s$. Thus, we have carried out the signal acquisition detection successfully.

The procedure described above is the processing procedure for a specific frequency bin of a specific satellite. To perform parallel processing for different carrier frequency bins of all satellites, supposing that there are I satellites and $(2K + 1)$ frequencybins, we repeat this process for each satellite and frequency bin and modify the sequence and parameters accordingly.

2.3 Analysis of Computation Cost

If we want to search for all possible code phases of a satellite at each frequency bin, for the serial method,

frequency-parallel method, matched-filter method, and compressed sensing method, correlation operations are needed first between the received signal and the correlation function of each branch. Because each correlation branch is composed of I and Q parts, each correlation branch requires $2N$ multiplication operations and $2(N-1)$ addition operations, where N is the number of samples in the integration period. Generally, $N \geq 2f_c \times 1ms$. N is at least 2046 for the C/A code of GPS.

The number of correlation branches in the conventional method is N , because all codes need to be searched. The number of branches in the compressed parallel correlation is reduced to P because compressed sensing can accept reduced-dimension measurements. In general, P is much smaller than N .

The total calculation cost of correlation is the product of the number of branches and the calculation cost of each branch. The conventional method requires $2N^2$ multiplication operations and $2(N-1)$ addition operations [6]. However, the compressed correlation requires $2N \times P$ multiplication operations and $2P(N-1)$ addition operations. If we ignore the calculation cost of generating the compressed correlation function by multiplying the reduced-dimension matrix and the correlation matrix in the real-time computation, the compressed acquisition method only includes the calculation of reconstruction, which has a cost of $O(ePN)$.

Thus, the total calculation cost of compressed acquisition is $3N \cdot P$ multiplication operations and less than $2P \cdot (N-1)$ addition operations (for $e \leq 1$). When $P < N$, the calculation cost of the compressed correlation acquisition method is far less than that of the conventional acquisition method.

2.4 Analysis of Detection Performance

$s_{i,k}$ is nonzero for h' satisfying $|h' T_s - \tau_{ni}| \leq T_s$, and $s_{i,k}$ is zero at other values. Comparing

$$s_{i,k}(h') = \frac{1}{2} A_i D_i \frac{T_{accu}}{T_s} S_a \left[\frac{1}{2} (k\Delta w - w_{di}) T_{accu} \right] \cdot \exp[-j(\hat{\phi}_{ni} - \hat{\phi}_{ni})]$$

with $z(i, k, \hat{\tau}_n) = \frac{1}{2} A_i D_i (nT_s) \frac{T_{accu}}{T_s} R_i(\hat{\tau}_n - \tau_{ni})$.

$$S_a \left[\frac{1}{2} (k\Delta w - w_{di}) T_{accu} \right] \exp[-j(\hat{\phi}_{ni} - \phi_{ni})]$$

we can see that the coefficient $R_i(\hat{\tau}_n - \tau_{ni})$ is the difference between $z(i, k, \hat{\tau}_n)$ and $s_{i,k}(h')$. $\hat{\tau}_n$ is estimated for an interval of T_s , and when $|\hat{\tau}_n - \tau_{ni}| \leq T_s$, the values of the two detection quantities are basically

the same. However, the detection quantity $z(i, k, \hat{\tau}_n)$ is calculated by accumulation, but the calculation of the detection quantity $s_{i,k}$ needs to be realized by reconstruction. Therefore, the reconstruction accuracy and success rate determine the differences in the detection performance and the success rate between the two methods.

The detection performances are basically equal provided that the reconstruction is completely accurate. In fact, the OMP method may have the problem of inaccurate support-set determination in the course of recovery. According to the study, there are two reasons why this problem could arise. One is due to the compressed sampling model: When the compression ratio is larger, the SNR loss in the recovery information is greater. Larger SNR loss causes greater recovery-amplitude error at the accurate position after the noise is mapped to the recovery vector, which makes the support-set determination difficult. The other reason is due to the non-orthogonality of the dictionary base: when the sampling compression ratio is larger, the ratio of cross-correlation to auto-correlation of dictionary bases will increase. Thus, the useful energy of the signal will be more easily mapped to the non-support set to form spurious noise. This also makes the support-set determination difficult. According to the above analysis, two aspects make it difficult to judge the support set of the useful signal, resulting in inaccurate signal acquisition results.

The relevant detailed derivation for the acquisition-detection success probability is very complicated [21]. After reasonable approximation, we roughly deduce that the useful signal obeys the distribution $N(1, \sigma_d^2)$ and the noise obeys the distribution $N(mean_{no-orth}, \sigma_f^2)$, where

$$\sigma_d^2 = e \frac{N}{P} \frac{1/1023 + 1/SNR}{f_s / f_c},$$

$$\sigma_f^2 = \sqrt{\frac{1/1023 + 1/SNR}{f_s / f_c} + \sigma_{no-orth}^2}, \text{ and } mean_{no-orth} \text{ and}$$

$\sigma_{no-orth}^2$ are, respectively, the mean and variance of the noise in measuring the non-orthogonality of the dictionary bases. Thus, the detection performance depends on the SNR, compression ratio N/P and non-orthogonality of the dictionary bases.

This study has found that the GPS acquisition-detection performance is affected by many factors. If we choose the appropriate measurement matrix and reconstruction algorithm, we can theoretically reconstruct the original signal with a probability of 100% under the condition of standard GPS SNR. However, due to the aforementioned reasons, this is not always the case. The detection probability of the proposed method is slightly lower than that of the conventional acquisition method.

3 Experimental Verification

3.1 Experiment Settings and Platform Construction

(1) For an instance of the actual data collected by a GPS receiver in Hainan at 13:53 on August 30, 2008, we carry out acquisition with compressed-processing software developed on the MATLAB platform. We present the 3-dimensional acquisition-result figures obtained by compressed acquisition processing for certain existing satellites and for certain non-existing satellites. By comparing them with the corresponding acquisition-result figures obtained by conventional acquisition methods, the effectiveness of the compressed acquisition method is validated.

(2) For purposes of analyzing the influence of different SNR signals on compressed acquisition performance and selecting an appropriate number P of correlation branches, we adopt the hardware simulator of IFEN Company to simulate the received multi-satellite signal. The simulated received GPS signal with controllable SNR and multi-satellite parameters is first frequency down-converted and sampled with hardware and then processed with compressed-processing software developed on the MATLAB platform.

3.2 Processing of Simulated Data

The IFEN simulator generates GPS RF signals of multiple satellites in a certain scene. The IF is 2.7 MHz after down conversion. The sampling rate of A/D is $f_s = 4.5\text{MHz}$, the period of the C/A code is 1 ms, the time of the correlation integral is $T_{\text{accu}} = 2\text{ms}$, and the number of samples in one integration interval is $N = 4500$. We set the normalized amplitude of Satellite No. 3 to one, the Doppler frequency w_{di} to $2\pi \times 3400$ Hz, and the search frequency interval Δw to $2\pi \times 500$ Hz. Therefore, the correct frequency bin is $k = 7$, the code phase delay at reference time t_{oi} is $\tau_{ni} = 23.4$ chips, and the carrier phase ϕ_{ni} is 0.14π .

We take the acquisition of Satellite 3 as an example to explain the compressed acquisition method. We perform despreading and demodulation of the sampled IF data with the C/A code of Satellite No. 3 and the carrier in frequency bin $k = 7$. The sparsity should be $e = 1$; $P \geq c \cdot e \cdot \log_2\left(\frac{N}{e}\right) = 12.13c$. In a real situation, due to the low SNR, P needs to be determined according to the real environment.

According to the simulation-environment settings described above, we perform the following experiments.

Experiment (1): We choose a random Gaussian measurement matrix and the OMP algorithm as the dimension-reduction matrix $A_{P \times N}$ and the reconstruction

algorithm. To explain the algorithm, we set a larger value of $e(e=5)$ to see how the recovered sparse elements are chosen. When $P = 700$ and $\text{SNR} = -16\text{dB}$, the reconstructed sparse vectors $s(h)$ are

$$s(103) = 0.5421e^{j0.0880\pi};$$

$$s(2011) = 0.2736e^{-j0.5995\pi};$$

$$s(2260) = 0.1649e^{j0.1246\pi};$$

$$s(3787) = 0.1174e^{-j0.8287\pi};$$

$s(3858) = 0.1735e^{-j0.8710\pi}$ and $s(q) = 0$ when $q \neq 103 \cdot 2011 \cdot 2260 \cdot 3787 \cdot 3858$.

The maximum amplitude value of $s(T_s), s(2T_s), \dots, s(NT_s)$ is $s(103) = 0.5421e^{j0.0880\pi}$. The detection threshold is set to 0.33. The amplitude of $s(103)$ is larger than this threshold, which indicates that the signal of Satellite 3 exists. The acquisition frequency bin is $k = 7$. We determined that $\hat{g} = 103$, so $|s(\hat{g})| = 0.5421$ indicates the relative amplitude of the signal and $\hat{g} = 103$ indicates that the delay of code phase of the signal is $103T_s$. Corresponding to a code-phase location of 23.42 chips, $103T_s$ is computed as $103/4.5\text{MHz} \cdot 1.023\text{MHz} = 23.42$ chips. The deviation between the estimate and τ_{ni} is very small, so the detection result is correct.

Thus, we have successfully carried out the acquisition detection of the signal.

Experiment (2): We choose a random Gaussian measurement matrix and the OMP algorithm as the dimension-reduction matrix and the reconstruction algorithm. Table 1, Table 2 and Table 3 show the successful acquisition times for 100 Monte Carlo experiments for SNRs of (-23~-14) dB and $P = 700, 1400, 2000$. We set $e = 1$. Note that if the deviation between the maximum-peak code phase and the correct code phase is smaller than half a chip, the acquisition is deemed successful.

From Table 2, we can see that for the same number of correlation branches P , the higher the SNR is, the better the effect of compressed-sensing reconstruction and the higher the success rate of acquisition. Comparing Table 3 with Table 4, for the same SNR, the larger the number of correlation branches P is, the better the effect of compressed-sensing reconstruction and the higher the success rate of acquisition. For a -15 dB SNR signal, $P = 2000$ is sufficient. Under a low SNR of -19 dB, the reconstruction effect is acceptable with $P = 2500$.

For different requirements of acquisition performance and computing-resource reduction, we can choose different types of dimension-reduction matrices, different reconstruction algorithms and different values of P according to compressed-sensing theory. The hardware-realization complexity is different.

Table 1. The successful acquisition times for different SNRs, P=700

SNR (dB)	-23	-22	-21	-20	-19	-18	-17	-16	-15	-14
Successful times	13	19	21	32	45	57	81	90	90	97

Table 2. The successful acquisition times for different SNRs, P=1400

SNR (dB)	-23	-22	-21	-20	-19	-18	-17	-16	-15	-14
Successful times	29	34	54	63	70	80	89	93	96	100

Table 3. The successful acquisition times for different SNRs, P=2000

SNR (dB)	-23	-22	-21	-20	-19	-18	-17	-16	-15	-14
Successful times	31	39	58	69	75	85	95	98	99	100

Table 4. The successful acquisition times for different SNRs, P=2500

SNR (dB)	-23	-22	-21	-20	-19	-18	-17	-16	-15	-14
Successful times	34	45	61	74	82	89	98	100	99	100

We see from the simulations above that when $N=4500$ and $P=2000$, a satisfactory acquisition effect in a low-SNR environment will be achieved with a Gaussian random matrix and the OMP reconstruction algorithm. To search all code phases of a certain satellite in a certain carrier frequency bin, the conventional acquisition method requires $2N^2 = 4.05 \times 10^7$ multiplication operations and $2N(N-1) = 4.05 \times 10^7$ addition operations for the correlation operation. However, the compressed correlation acquisition method only requires approximately $2N \cdot P = 2.7 \times 10^7$ multiplication operations and $3P(N-1) = 2.7 \times 10^7$ addition operations. The calculation cost is less than 67% of that of the serial acquisition method.

3.3 Processing the Actual Data

We will process the actual data collected by the GPS receiver in Hainan at 13:53 on August 30, 2008. The acquisition results obtained by conventional acquisition and compressed acquisition methods for satellite No. 16 and satellite No. 4 are shown in Figure 2、Figure 3、Figure 4 and Figure 5. The 3-dimensional acquisition result obtained by compressed acquisition processing is the reconstructed correlation values, which are reconstructed according to the estimated sparse vector. The reconstructed correlation values correspond to correlation values obtained by a conventional correlator after the IF signal was disperse and demodulated. Both methods show that satellite No. 16 exists and satellite No. 4 does not exist. Through comparison, we find that a more obvious peak exists in the compressed acquisition of satellite No. 16. This is because only the detected sparse element is used to reconstruct the correlation value. When a satellite does not exist, taking satellite No. 4 as an example, we cannot detect any $s_{4,k}(h)$ that exceeds the threshold. Therefore, all the entries of the sparse vector are taken

as zero, so the reconstructed correlation values for satellite No. 4 are all zero. The validity of the method is demonstrated.

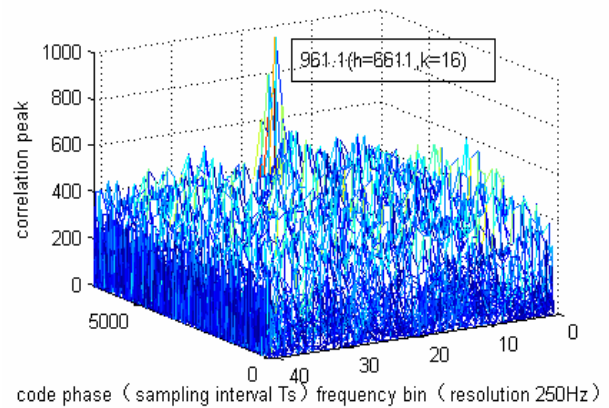


Figure 2. The 3-dimensional acquisition result of the existing satellite No. 16 obtained using the conventional acquisition method

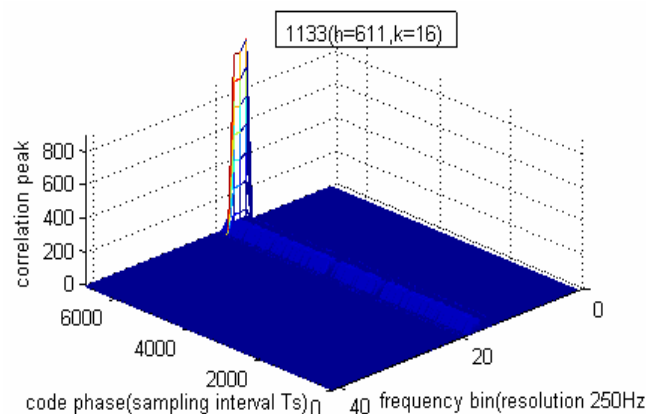


Figure 3. The 3-dimensional acquisition result of the existing satellite No. 16 obtained using the compressed acquisition method

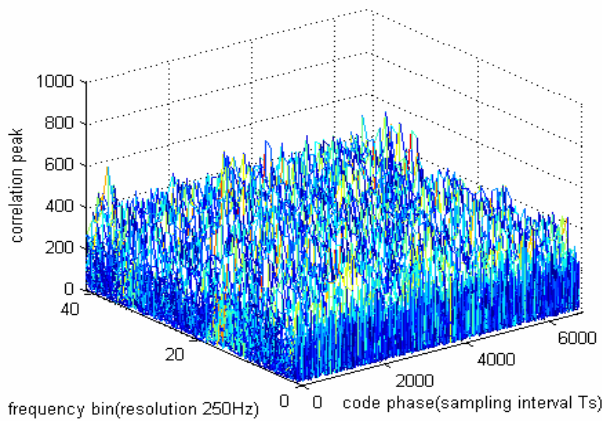


Figure 4. The 3-dimensional acquisition result of the existing satellite No. 4 obtained using the conventional acquisition method

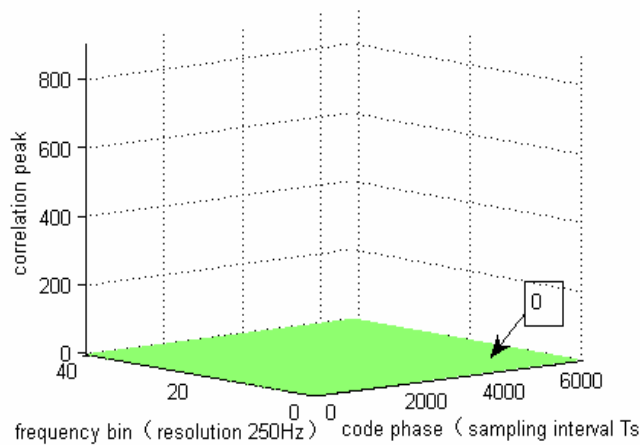


Figure 5. The 3-dimensional acquisition result of the existing satellite No. 4 obtained using the compressed acquisition method

Figure 6 adopts a 3-dimensional figure to show the acquisition result for multiple satellites and frequency bins, obtained with the compressed acquisition method. The result shows that four satellites are acquired and arranged in the order 23, 16, 13 and 6 according to the signal intensity. The largest acquisition-peak value of satellite No. 6 is 998.5, and it appears at the 21st frequency bin and the code phase of the 3195th sampling interval. The largest acquisition-peak value of satellite No. 13 is 1042.0, and it appears at the 26th frequency bin and the code phase of the 6803rd sampling interval. The largest acquisition-peak value of satellite No. 16 is 1121.0, and it appears at the 16th frequency bin and the code phase of the 6611th sampling interval. The largest acquisition-peak value of satellite No. 23 is 1134.0, and it appears at the 16th frequency bin and the code phase of the 1989th sampling interval.

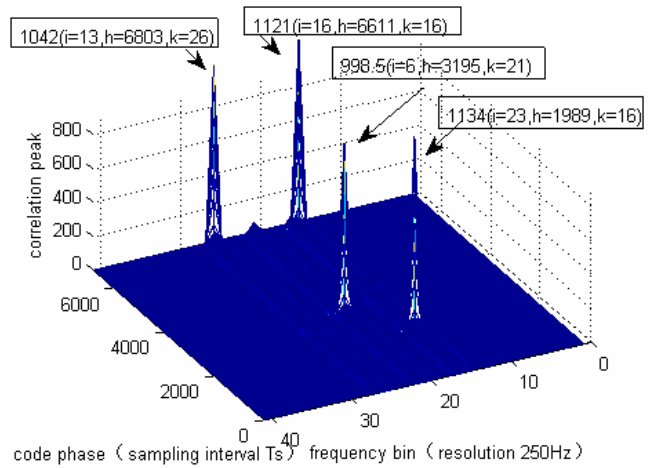


Figure 6. The 3-dimensional acquisition result of all the satellites, obtained with the compressed acquisition method

Figure 7 adopts a 3-dimensional figure to show the acquisition result for multiple satellites and frequency points, obtained with the conventional acquisition method. The result shows that four satellites are acquired, including the satellites numbered 23, 16, 13, and 6. The largest acquisition-peak value of satellite No. 6 is 671.5, and it appears at the 21st frequency bin and the code phase of the 3195th sampling interval. The largest acquisition-peak value of satellite No. 13 is 813.3, and it appears at the 26th frequency bin and the code phase of the 6803rd sampling interval. The largest acquisition-peak value of satellite No. 16 is 961.1, and it appears at the 16th frequency bin and the code phase of the 6611th sampling interval. The largest acquisition-peak value of satellite No. 23 is 975.0, and it appears at the 16th frequency bin and the code phase of the 1989th sampling interval.

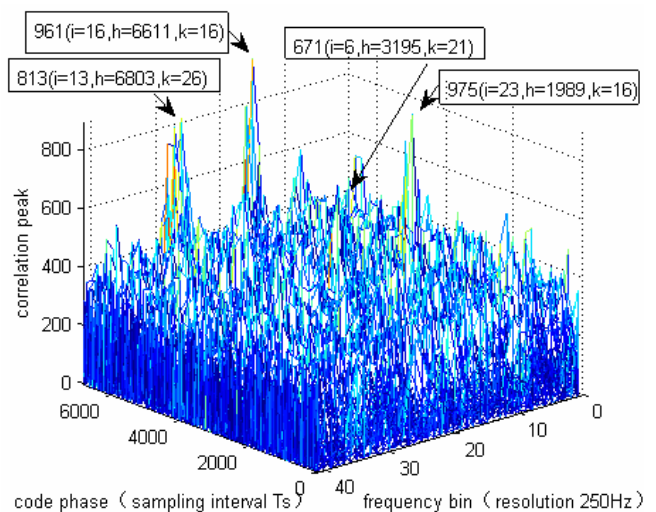


Figure 7. The 3-dimensional acquisition result of all the satellites, obtained with the conventional acquisition method

The results show that the acquisition result obtained with the compressed acquisition method proposed in this paper is completely in accordance with that obtained with the conventional acquisition method. Similar to the conventional acquisition method, when a low-probability incorrect acquisition appears, we can realize reliable acquisition validation by additionally processing data of a few more milliseconds.

4 Conclusions

In this paper, the GNSS acquisition method based on compressed sensing is studied. We build the model of the compressed sensing measurements and the sensing matrix and design the acquisition-processing method suitable for the GNSS receiver. Then we use OMP to reconstruct key acquisition information. Through analysis and experiments, we see that this method is feasible. The reconstruction algorithm, under certain conditions, has the problem of inaccurate support-set determination, which influences the detection performance. According to the theoretical analysis, the detection performance is mainly related to the SNR, compression ratio, degree of dictionary-base non-orthogonality and other conditions. Although the detection performance is slightly lower than that of the conventional acquisition method, when using the correlation structure in the analog domain, the compressed acquisition structure can greatly reduce the computation and sampling rate in the digital part, which reduces the power consumption. The simulations show that with a moderate sampling rate and an SNR of -16 dB, the computational cost is less than 67 percent of that of the serial acquisition method. When the sampling rate is higher, the computation-reduction effect will be more obvious. For different requirements of detection performance and computing-resource reduction, we can choose different dimension-reduction matrices (the complexity of the hardware is different), reconstruction algorithms, values of P , etc. according to compressed-sensing theory. It is a good choice for GNSS acquisition.

Later we could study how to design a more reasonable measurement scheme to further reduce the computation cost, and also study the multiple testing problem to validate acquisition state.

Acknowledgments

This work was supported by the Natural Science Foundation of Beijing (4172021), the Importation and Development of High-Caliber Talents Project of Beijing Municipal Institutions (CIT & TCD201704064), Science and technology development plan of Beijing Education Commission (KM201711232010), Key research cultivation projects of BISTU (5221824108), Beijing Information Science and Technology

University's funding for science and technology innovation service capability project (71F1810921), National Natural Science Foundation Project (61302073), Projects funded by the Beijing Natural Science Foundation (Z160002).

References

- [1] E. D. Kaplan, C. J. Hegarty, *Understanding GPS: Principles and Applications*, Artech House, 2006.
- [2] J. Yang, T. Jin, Z. Huang, H. Qin, Multi-signal Components Combining Acquisition Method based on Padding Zero for TD-AltBOC, *Journal of Harbin Engineering University*, Vol. 35, No. 11, pp. 1427-1433, November, 2014.
- [3] L. Zheng, Z. You, G. Zhang, L. Ma, S. Zhao, Study on Fast GNSS Signal Acquisition in GNSS Receiver, *Chinese Journal of Scientific Instrument*, Vol. 35, No. 4, pp. 807-813, April, 2014.
- [4] L.-y. Zhang, *Research on Acquisition-tracking Algorithm and Anti-jamming Performance for BD-II Signal*, Master Thesis, Xidian University, Xi'an, China, 2014.
- [5] J. Yuan, S. Ou, Study on Parallel Acquisition Algorithm for GPS Receiver, *Journal of Chongqing University of Posts and Telecommunications (Natural Science Edition)*, Vol. 25, No. 4, pp. 470-474, August, 2013.
- [6] Z.-q. Wu, *Acquisition Algorithm Research and FPGA Implementation of GNSS Receiver*, Master Thesis, Beijing Telecommunication University, Beijing, China, 2011.
- [7] X.-m. Tang, J. Pang, Y.-b. Huang, F.-x. Wang, Optimization of XFAST Design, *Journal of Central South University (Science and Technology)*, Vol. 45, No. 4, pp. 1113-1118, April, 2014.
- [8] C. Liu, J. Zhang, Y. Zhu, Q. Pan, Analysis and Optimization of PMF-FFT Acquisition Algorithm for High-dynamic GPS Signal, Master Thesis, *Cybernetics and Intelligent Systems (CIS)*, Qingdao, China, 2011.
- [9] D. L. Donoho, Compressed Sensing, *IEEE Transactions on Information Theory*, Vol. 52, No. 4, pp. 1289-1306, April, 2006.
- [10] J. Jin, Y.-t. Gu, S.-l. Mei, An Introduction to Compressive Sampling and Its Applications, *Journal of Electronics & Information Technology*, Vol. 32, No. 2, pp. 470-475, February, 2010.
- [11] H. Rauhut, K. Schnass, P. Vandergheynst, Compressed Sensing and Redundant Dictionaries, *IEEE Transactions on Information Theory*, Vol. 54, No. 5, pp. 2210-2219, May, 2008.
- [12] R.-z. Zhao, R.-q. Wang, F.-z. Zhang, Y.-g. Cen, S.-h. Hu, Research on the Blocked Ordered Vandermonde Matrix Used as Measurement Matrix for Compressed Sensing, *Journal of Electronics & Information Technology*, Vol. 37, No. 6, pp. 1317-1322, June, 2015.
- [13] W. Dai, O. Milenkovic, Subspace Pursuit for Compressive Sensing Signal Reconstruction, *IEEE Transactions on Information Theory*, Vol. 55, No. 5, pp. 2230-2249, May, 2009.

[14] X. Li, A. Rueetschi, Y. C. Eldar, A. Scaglione, GPS Signal Acquisition via Compressive Multichannel Sampling, *Physical Communication*, Vol. 5, No. 2, pp. 173-184, June, 2012.

[15] S. H. Kong, A Deterministic Compressed GNSS Acquisition Technique, *IEEE Transactions on Vehicular Technology*, Vol. 62, No. 2, pp. 511-521, February, 2013.

[16] J. Liu, B.-g. Cai, Y.-h. Wen, J. Wang, Integrating DSRC and Dead-reckoning for Cooperative Vehicle Positioning under GNSS-challenged Vehicular Environments, *International Journal of Ad Hoc and Ubiquitous Computing*, Vol. 19, No. 1/2, pp. 111-129, 2015.

[17] Q. Wang, G. Qu, Restricted Isometry Constant Improvement based on a Singular Value Decomposition-weighted Measurement Matrix for Compressed Sensing, *IET Communications*, Vol. 11, No. 11, pp. 1706-1718, August, 2017.

[18] D. Needell, J. A. Tropp, CoSaMP: Iterative Signal Recovery from Incomplete and Inaccurate Samples, *Applied and Computational Harmonic Analysis*, Vol. 26, No. 3, pp. 301-321, May, 2009.

[19] J. Li, Q. Wang, Y. Shen, Near Optimal Condition of OMP Algorithm in Recovering Sparse Signal from Noisy Measurement, *Journal of Systems Engineering and Electronics*, Vol. 25, No. 4, pp. 547-553, August, 2014.

[20] M. Usman, C. Prieto, F. Odille, D. Atkinson, T. Schaeffter, P. G. Batchelor, A Computationally Efficient OMP-based Compressed Sensing Reconstruction for Dynamic MRI, *Physics in Medicine and Biology*, Vol. 56, No. 7, pp. 99-114, April, 2011.

[21] A. Aissaoui, Z. Hammoudi, A. Farrouki, Adaptive Pseudo-noise Code Acquisition Scheme using Automatic Censoring for DS/SS Communication in Frequency-selective Rayleigh Fading Channel, *IET Communications*, Vol. 2, No. 2, pp. 359-365, February, 2008.



Minling Zhu works in School of Computer, Beijing Information Science and Technology University as an associate professor. In 2012, she graduated in Beihang University in China for Ph.D., majored in Auto Control. Now her research interests focus on AI and the Embedding System.

Biographies



Yanxin Yao received her bachelor's degree and doctor's degree at Jilin University and Beihang University in 2005 and 2009, respectively. She is now an associate professor at Beijing Information and Science Technology University. About 30 academic papers have been published. Her main research interest is in compressed sensing and intelligent information processing, etc.